Available online at www.sciencedirect.com
ScienceDirect

Current Applied Physics 7 (2007) 305–313

Current Applied Physics
An official journal of the KPS

www.elsevier.com/locate/cap
www.kps.or.kr

Structural and electrochemical characterization of Ni nanostructure films on steels with brush plating and sputter deposition

B. Subramanian *, S. Mohan, Sobha Jayakrishnan, M. Jayachandran

Central Electrochemical Research Institute, Karaikudi 630 006, India

Received 15 May 2006; accepted 14 September 2006
Available online 7 November 2006

Abstract

Layers of nickel were coated on low carbon steel substrates applying both brush plating and DC magnetron sputtering techniques. X-ray diffraction analysis showed a preferential orientation along (111) for both sputter deposited and brush plated Ni nanostructure coatings. The sputtered Ni film showed better crystallinity as observed from XRD compared to brush plated Ni film on steel on account of the favorable conditions for grain growth in sputtering. SEM analysis indicated that the coatings are very regular without pores, with columnar structure for the sputter deposited Ni coatings. AFM was also applied for surface topography examination. Microhardness value was found to be higher for sputtered Ni film. Corrosion performance of these nanostructured Ni coatings were evaluated using electrochemical techniques and observed that the corrosion resistance of brush plated Ni film sample was significantly higher than that of the sputtered Ni film.

© 2006 Elsevier B.V. All rights reserved.

PACS: 81.15.-z; 82.45.Mp; 81.15.Cd

Keywords: Nickel deposition; Brush plating; Magnetron sputtering; Corrosion resistance

1. Introduction

Nickel and nickel based materials have received more interests recently for application of structural components in MEMS industries i.e. micro switches, accelerometers and also in the basic search [1]. Nickel coatings of various thickness can be employed as protective layers to improve corrosion resistance, wear resistance and hardness of steels and other alloys [2,3]. Electroless nickel films are used as the over coat of the titanium head of golf clubs for wear resistance improvement and also for parts of rockets, aircrafts automobile and industrial machines [4]. In general, 5–40 μm thick nickel coating is applied for decorative purposes [5].

The brush plating technique, different from conventional plating, is an electrochemical process conducted with an electrolyte applied to the substrate by a so-called brush to form the adherent deposit [6]. Most metals used in conventional electrodeposition can be brush plated; the main applications are for repair and resizing purposes. Nano-Al_2O_3/Ni brush plated composite coatings were deposited by co-deposition of Al_2O_3 nanoparticles with Ni metal matrix during brush plating [6]. Hui et al., have reported the corrosion resistance of brush plated Ni–Fe–W–P films [7].

Due to its portability, flexibility and easy to operate, brush plating has found increasing use in industry. Dini [8] summarized quantitative property data on a variety of brush plated deposits, which offer promise in applications involving wear and/or corrosion resistance. Subramanian et al. [9] adopted brush plating technique to prepare tin selenide thin films on tin oxide coated conducting glass substrates at room temperature.

Sputtering is one of the physical vapor deposition (PVD) techniques which can be employed to deposit Ni coatings in place of solution method on account of its good

---

* Corresponding author. Tel.: +91 4565 227555; fax: +91 4565 227779.
E-mail address: tspsenthil@yahoo.com (B. Subramanian).

1567-1739/$ - see front matter © 2006 Elsevier B.V. All rights reserved.
doi:10.1016/j.cap.2006.09.003

control of experimental parameters such as thickness and composition. The nickel based nanocrystalline coatings synthesized by sputter deposition on stainless steel showed a large increase of the wear resistance [10]. Wear behavior in TiN coatings modified by an electroless Bi interlayer on mild steel was reported by Doong et al. [11] and Sing et al. [12]. Nanostructure films, consisting of TiN and Ni, were obtained by filtered vacuum arc deposition [13]. The electroless nickel–phosphorous plating with differing phosphorous contents was employed as an interlayer to modify the properties of CrN hard coating on mild steel [14]. Detailed simulations of low energy, normally incident Xe^+ ion sputtering of low index nickel surfaces are reported [15]. Milkani et al. [16], have reported the effect of DC bias voltage on the deposition rate for Ni thin films by RF-DC coupled unbalanced-magnetron sputtering.

Although both brush plating and magnetron sputtering of nickel thin films on steels have been developed, there is no direct comparison of these two types of thin films synthesized simultaneously. In this investigation, a comparison was made between brush plated and sputtered nickel coatings on steel substrates with respect to microstructure, surface morphology and corrosion properties.

2. Experimental

2.1. Surface preparation of substrates

Nickel coatings were fabricated on mild steel substrates. The composition of the mild steel substrate used in this study is shown in Table 1. Coupons of the substrate was cut to an appropriate size of 75 × 25 mm and ground with SiC sand paper to remove the heavy oxide and contamination. The ground substrates were then polished with 1 μm alumina powders to obtain smooth surfaces. The polished substrates were degreased with acetone and then cathodically electro cleaned in alkali solution containing sodium hydroxide and sodium carbonate for 2 min at 70 °C, followed by rinsing with distilled water. The brush plating or sputtering Ni layers were then fabricated on the smooth and clean mild steel substrates.

Table 1
Specified composition of carbon steel substrate

%C	%Mn	%S	%P	%Fe
0.063	0.23	0.03	0.011	Balance

2.2. Brush plating of nickel

Brush plating equipment includes power packs, solutions and plating tools, anode covers and auxiliary equipment. Microprocessor controlled Selectron Power Pack Model 150A – 40 V was used to transform AC current to DC current. The schematic of the brush plating system is given in Fig. 1. The power pack has two leads, one is connected to the plating tool and the other is connected to the workpiece to be plated. The anode is covered with an absorbent material which holds the solution. The operator dips the plating tool in the solution and then brushes it against the surface of the workpiece that is to be finished. When the anode touches the work surface a circuit is formed and deposit is produced. The electrolyte bath (Table 2) similar to Watt's bath contained 240 g/l nickel sulphate, 40 g/l nickel chloride and 30 g/l boric acid. The pH and temperature was maintained at 4.0 and 28 °C (RT). Fig. 2 shows a cyclic voltammogram obtained for the bath used for brush plating of Ni films. It is observed that Ni deposition takes place at −1.0 V and two stripping peaks are noted at +0.25 and +0.75 which indicates the bath behaves as that of the usual watt's bath.

2.3. Sputter deposition of nickel

The layers of Ni were deposited on well cleaned mild steel substrates with a dc magnetron sputter deposition unit

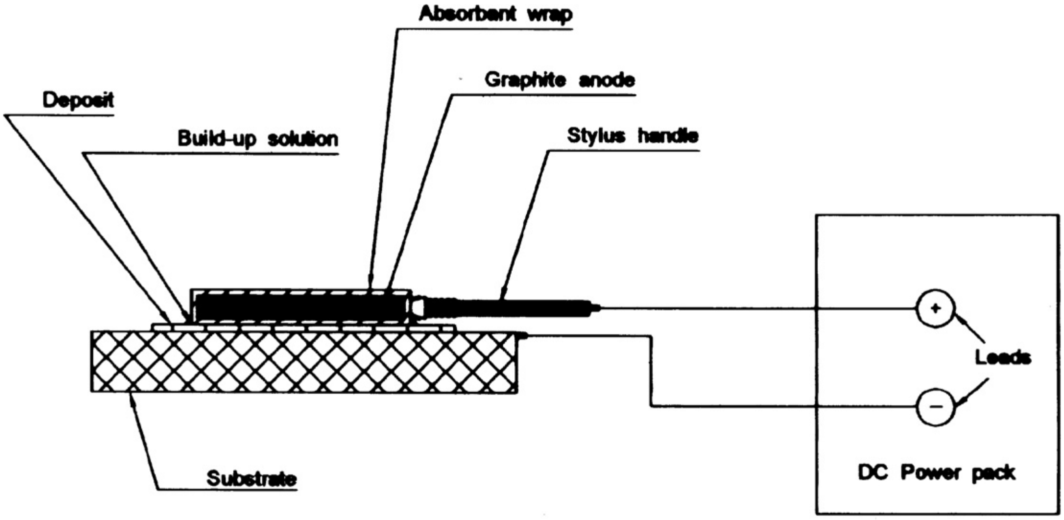

Fig. 1. Schematic of brush plating process.

Table 2
Optimized parameters for Ni brush plating

Parameter	Value
Nickel sulphate	240 g/l
Nickel chloride	40 g/l
Boric acid	30 g/l
Temperature	28 °C
pH	4
Plating voltage	2 V
Duration	30 min

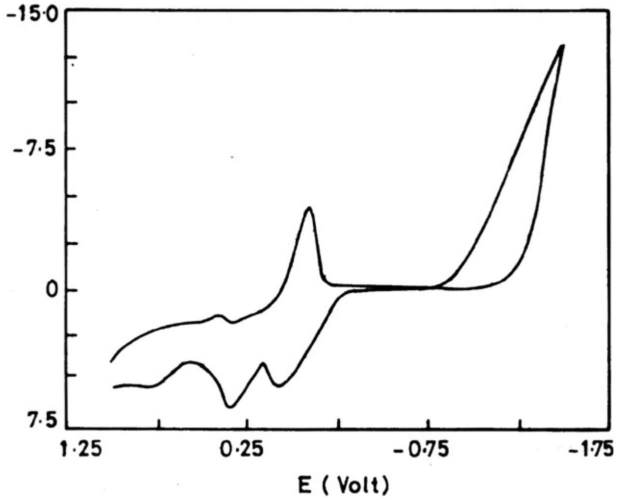

Fig. 2. Cyclic voltammogram of Ni brush plating bath.

AVS 114D. The base vacuum of the chamber was below 1×10^{-6} Torr at the substrate temperature of 100 °C. A high purity argon was fed into the vacuum chamber for the plasma generation. The substrates were etched for 34 min at a dc power of 50 W and an argon pressure of 10 mTorr (1.33 Pa). (A high purity >99.999% Ni target 7.5 cm in diameter was used as cathode). The deposition parameters for Ni sputtering are summarized in Table 3.

2.4. Characterization

The deposited films were analyzed for crystallographic structure with a diffractometer using CuKα line. The microstructure of the coatings was examined using a Hitachi S 3000H scanning electron microscope and a molecular imaging Atomic Force Microscope. Micro hardness of the nickel coated steels was evaluated by using a DM-400 micro hardness tester from LECO with Vickers indenters. A dwelling time of 15 s and a load of 25 g were used for the measurement. Porosity of the coatings was measured using Ferroxyl test. The test solution was prepared by dissolving 10 g of agar, 10 g of sodium chloride (NaCl), and 1 g of potassium ferricyanide $[K_3Fe(CN)_6]$ in 1 L of warm deionized water. The surface of the coatings were cleaned and degreased with acetone. The test solution was heated to 93 °C to liquefy. A piece of filter paper was dipped into the solution (the excess solution was allowed to drain off) and then applied the wet paper to the test area and allowed to remain undisturbed for few minutes. At the end of the test period the filter paper was removed and tested.

Table 3
Deposition parameters for Ni sputtering

Parameter	Value
Ultimate vacuum	1×10^{-6} mbar
Operating vacuum	3×10^{-3} mbar
Ar gas pressure	2–3 kg/cm^2
Ar gas flow rate	12 cc/min
Power	82 W
Distance between target and substrate	60 mm
Substrate temperature	100 °C

Electrochemical polarization studies were carried out using BAS IMG Electrochemical analyzer. Experiments were conducted using the standard three-electrode configuration, with a platinum foil as a counter electrode saturated calomel electrode as a reference electrode and the sample as a working electrode. Specimen (1.0 cm^2 exposed area) was immersed in the test solution of 3.5% NaCl. Experiments were carried out at room temperature (28 °C).

3. Results and discussion

3.1. Deposition rate, adhesion and microhardness

The film thickness as a function of processing time of brush plated Ni films is shown in Fig. 3. The thickness of the nickel films exhibits a parabolic relationship with plating time. The parabolic relationship may reflect a diffusion controlled mechanism. The deposition rate depends on the arrival rate of the reagent onto the specimen surface. The film thickness as a function of the deposition time for sputter deposited nickel films is shown in Fig. 4. For the sputter deposited Ni films, it was achieved by the bombardment of Ar^+ with the Ni target. The thickness vs time diagram shows a linear relationship. For a coating thickness of up to 1 μm, it is observed that the brush Ni plating provided a deposition rate approximately ten times that from sputtering which is generally a slower process than plating.

The microhardness values of 180 Hv and 143 Hv were measured for the sputtered and brush plated Ni film respectively. A relatively higher microhardness is observed for sputter Ni coated steels as a result of high residual stresses from sputtering process.

3.2. XRD analysis

The X-ray diffraction patterns obtained for the brush plated and sputter deposited nickel films are shown in Fig. 5a and b respectively. For the brush plated nickel coatings, preferentially oriented broad peak can be observed at $2\theta = 44.9°$, corresponding to Ni (1 1 1) planes. For the sputter deposited nickel coatings, the XRD clearly show sharp Ni peaks indicating better crystalline nature. The difference in crystallization tendency may be contributed

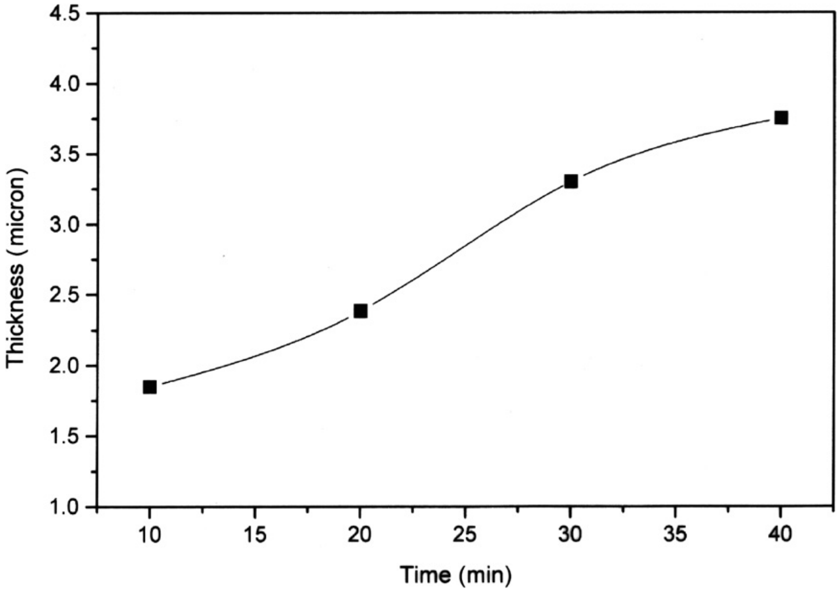

Fig. 3. Deposit thickness of the brush plated Ni film as a function of plating time.

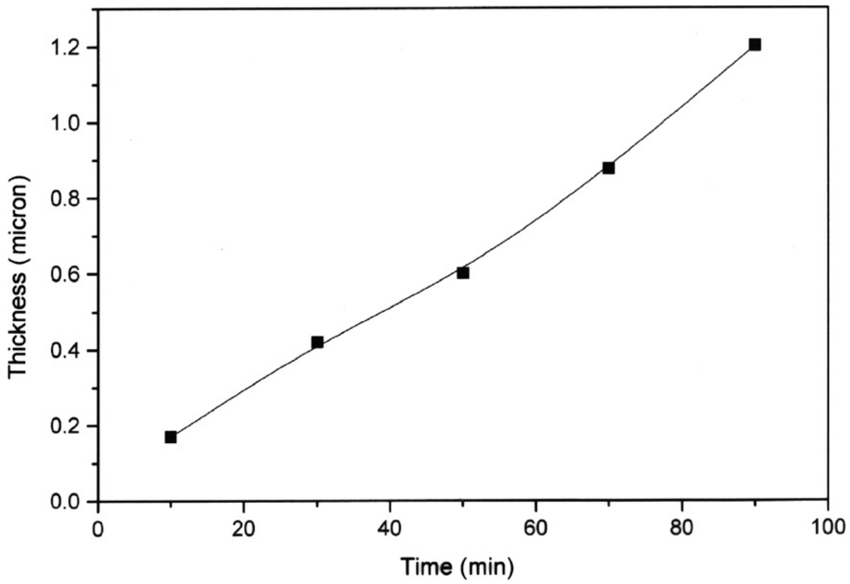

Fig. 4. Deposit thickness of the sputtered Ni film as a function of sputtering time.

to the different mechanism of these two coating techniques. In sputter deposition, nickel atoms are bombarded down continuously to the heated substrates with relatively high energy and spread randomly on the surface. The microstructure of the sputter deposited Ni coatings was expected to be columnar grains separated by dense intercrystalline boundaries as reflected by the sharp diffraction peaks in the XRD pattern [4].

In the case of brush plating technique, the temperature was kept at 28 °C which is very low compared to the sputtering process, resulting in the slow rate of deposition of the Ni grains. The low energy involved in the brush plating process impeded the growth of nickel grains.

The grain size of these coatings could be determined by the equation

$$D = 0.94\lambda/\beta\cos\theta, \tag{1}$$

where D is the grain size, β is the full width at half maximum (FWHM) of the diffraction peak, λ is the wavelength of the incidental CuKα X-ray (1.514 Å), and θ is the diffraction angle. Based on Eq. (1), the estimated grain size of the (1 1 1) oriented Ni was around 30 nm for the sputtered Ni and 25 nm for the brush plated Ni coatings. Such a small grain size contributes to the smooth surface morphology and also may have a beneficial effect on the improvement of the microhardness of the coating [17]. Also

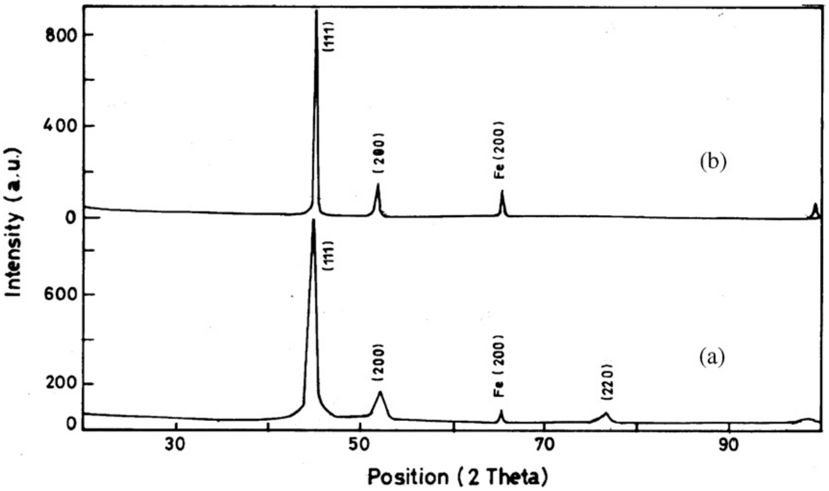

Fig. 5. X-ray diffractogram of the (a) brush plated and (b) sputtered Ni film.

the grain size reduction to the nanometer range results in considerable improvement in their resistance to localized corrosion [18].

The strain (ε) was calculated from the slope of the $\beta\cos\theta$ vs $\sin\theta$ plot using the relation [19]

$$\beta = \lambda/D\cos\theta - \varepsilon\tan\theta. \tag{2}$$

The dislocation density (δ), [19] defined as the length of the dislocation per unit volume of the crystal, was calculated from the formula

$$\delta = 1/D^2. \tag{3}$$

It is observed from the Table 4 that sputtered Ni coatings have larger crystallite size than that of the brush plated Ni coatings. Since crystallite size and dislocation density are inversely related, the dislocation density decreases with increase of the crystallite size. It is also noted that the strain is more in the case of sputtered coatings. During sputtering of Ni, argon ions in the plasma were attracted to the target at high speeds and knocked Ni atoms down through a momentum exchange process. Sputtered Ni atoms with relatively high momentum traveled to the substrate surface and adsorbed on it. Depending on the adsorbing, the substrate temperature and the crystal structure of the adsorbing surface, Ni films of various structures would grow. Internal residual stresses could be built up in the deposited Ni films on the low carbon steel substrate due to lattice mismatch between the Ni structure and the substrate surface.

Table 4
Parameters derived from XRD analysis

Sample	d (nm)	D (nm)	δ (10^{14} lin m^{-2})	ε (10^{-4} lin^{-2} m^{-4})
Sputtered Ni	2.037	31.0	10.4	17.5
	1.017	28.3	12.4	19.5
Brush plated Ni	2.037	25.6	15.3	16.4
	1.764	25.7	15.2	15.1

3.3. Microstructure analysis

3.3.1. SEM analysis

Fig. 6a and b show the scanning electron micrographs of the brush plated Ni and sputter deposited Ni coatings respectively. It can be viewed from the figures that a very smooth surface morphology was observed for the Ni deposits obtained by both brush plating and sputtering. The columnar structure was observed for the sputter deposited Ni coatings. The porosity of nickel coating is strictly related to the thickness and thick Ni coatings are involved in anticorrosive applications. Because, the initiation and continuation of corrosion at the surface of underlying metal strongly depends on the barrier efficiency of the coating against the attack of corrosive environment. Ferroxyl test also showed no blue spots on the soaked filter paper with 1.2 μm sputtered Ni film and 4.0 μm brush plated Ni film.

3.3.2. AFM analysis

The surface topography of these Ni coatings was studied using Atomic force microscopy (AFM). The basic study comprised a 3D representation for a scanned area of 5 × 5 μm and the section analysis method that allows the determination of the profile of the samples with a line drawn over the surface which is shown in Fig. 7a and b. On Ni sputter coated mild steel surface, we can identify the effects of the mechanical polishing of the substrate as linear marks (channels) and small clusters. Whereas on brush plated Ni coatings on mild steel, the coverage of grains with few clusters on the entire surface were observed.

From the horizontal cross section analysis, the minimum and maximum globule size was estimated to be in the range of 50–200 nm for the brush plated Ni coating and in the range of 50–100 nm for the sputter deposited Ni coatings on mild steel were observed. There are some shallow valleys of around 10 nm depth was observed in sputtered Ni coatings.

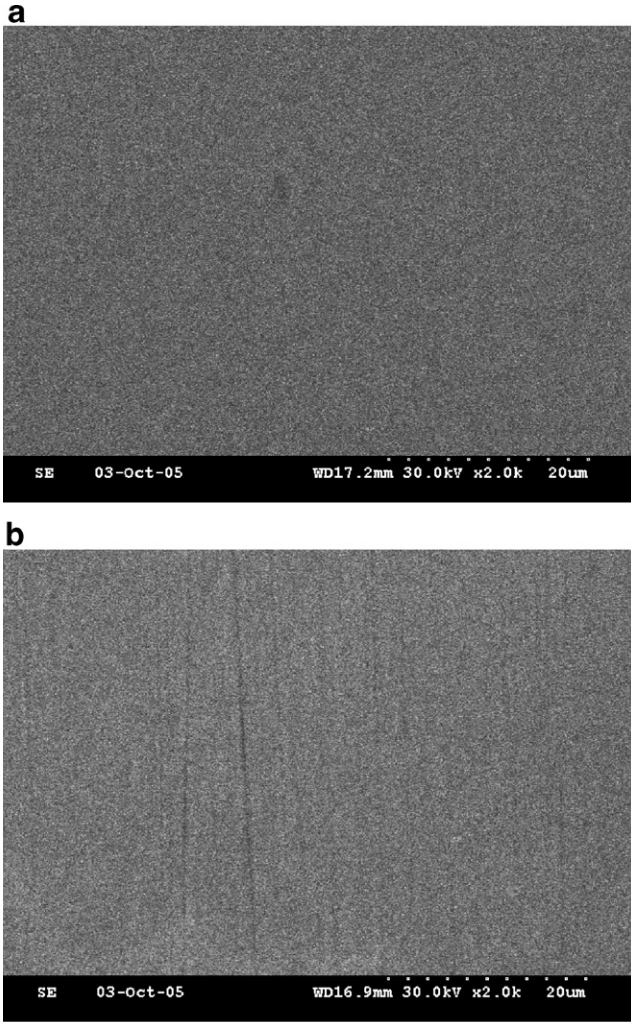

Fig. 6. Scanning electron micrograph of the (a) brush plated and (b) sputtered Ni film.

Roughness analysis of these coating was carried out and the value of the mean roughness R_a was calculated as the deviations in height from the profile mean value [12].

$$R_a = \frac{1}{N} \sum^{N} |Z_i - Z|, \tag{4}$$

where Z is defined as the sum of all height values divided by the number of data points (N) in the profile. The roughness value, estimated from these images using Eq. (4) was 12.65 nm for the brush plated Ni coatings and 12 nm for the sputter deposited Ni coatings. Which shows that both brush plating and sputtering produced smooth Ni films.

3.4. *Potentiodynamic polarization and AC impedance spectroscopy*

The principal aim of this investigation was to study surface degradation resulting from electrochemical processes, and this necessitated an analysis of the surface deposit left after electrochemical reactions. The potentiostatic polarization experiments provided some idea of the electrochemical activity of the material. However, this necessitated scanning across a wide range of electrode potentials so that the surface of the material at the end of such polarization was the result of cumulative effects at different potentials. To analyse the surface, the material was subjected to potentiostatic polarizations, one specified potential being impressed on the material at a time. The potentials were either anodic or cathodic with respect to the primary electrochemical process occurring on the surface as indicated by the potentiostatic polarization curves. The current and potential of the corroding electrode is related by

$$I = i_{\mathrm{corr}}(\mathrm{e}^{2.3\eta/b_a} - \mathrm{e}^{-2.3\eta/b_c}), \tag{5}$$

where I_{corr} – corrosion current; η – overpotential ($E - E_{\mathrm{corr}}$), b_a and b_c are the anodic and cathodic Tafel slopes.

At high over potentials i.e.

$$\begin{aligned} &\eta \gg RT/F, \\ &i_a = i_{\mathrm{corr}}\mathrm{e}^{2.3\eta/b_a}, \\ &\log i_a = \log i_{\mathrm{corr}} + \eta/b_a. \end{aligned} \tag{6}$$

In the plot of η vs $\log i$ extrapolation of linear line to corrosion potential gives a straight line and the slope gives both b_a and b_c and the intercept gives the corrosion current.

Typical polarization curves obtained for the corrosion behavior of the Ni sputtered mild steel samples are shown in Fig. 8. Table 5 includes the values of the corrosion potential (E_{corr}), the corrosion current density (I_{corr}), the anodic and cathodic Tafel slopes during polarization in 3.5% w/v NaCl and the corrosion rate. E_{corr} and I_{corr} values improve (a less negative value of E_{corr} and lower value of I_{corr} signifies an improvement in corrosion) for brush plated Ni than for sputtered Ni and bare mild steel substrates. This may also be due to less porous nature of the brush plated Ni coatings thereby increase in nucleation sites.

The same three electrode cell assembly, as used for the potentiodynamic polarization experiments, was employed for the AC impedance investigations. Impedance measurements were made at open circuit potential (OCP) applying an AC signal of 10 mV in the frequency range 10 Hz to 1 MHz. The Nyquist plots for the samples used for corrosion tests in 3.5% w/v NaCl solution are shown in Fig. 9. The equivalent circuit for a corroding metal which has both anodic and cathodic reaction activation controlled may be represented as in Fig. 10.

The double layer capacitance C_{dl} value is obtained from the frequency at which Z imaginary is maximum [20]

$$\omega(Z_{(\mathrm{im})}\max) = 1/C_{\mathrm{dl}}R_{\mathrm{ct}}. \tag{7}$$

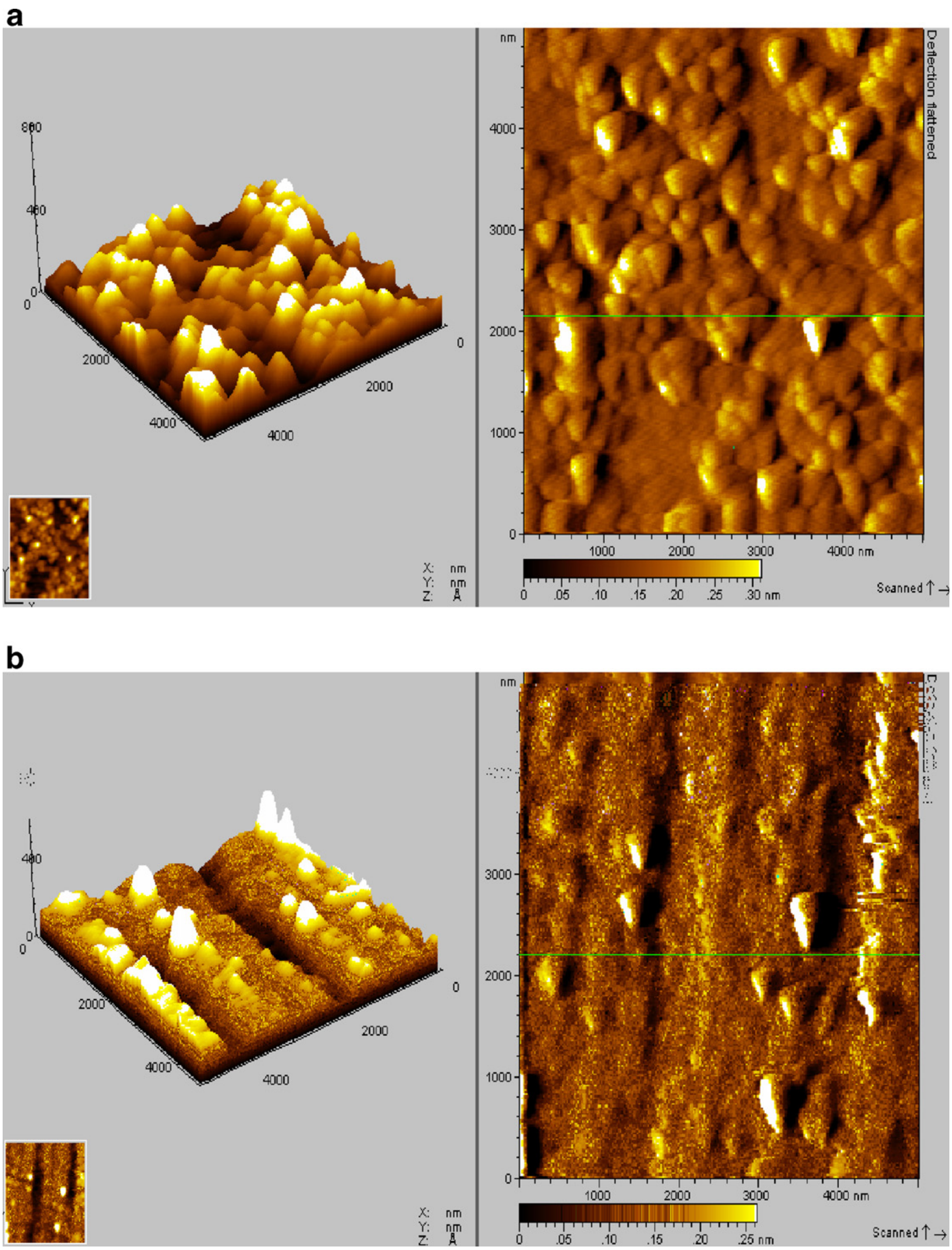

Fig. 7. AFM images (scan size 1 × 1 μm) showing the topography of Ni film (a) brush plated and (b) sputtered.

The increase in R_{ct} values and decrease in C_{dl} values as shown in Table 6 for the brush plated Ni film confirm the better corrosion resistance of these systems compared to sputtered Ni film and bare mild steel substrate. The corrosion rate (CR) is expressed in mills per year [20].

$$\mathrm{CR} = 0.1288 \times i_{\mathrm{corr}} \times w/\rho, \tag{8}$$

where i_{corr} is the corrosion current in amp/cm^2, w is the equivalent weight of metal, ρ is the density.

The corrosion rate observed on brush plated Ni film sample was significantly lower than that of the sputtered Ni film exhibiting the lowest corrosion rate of brush plated Ni film of all the three samples.

Brush plated nickel composite coatings have widespread use in engineering, which conventionally have particles of a diameter ranging between 1 and 100 μm. There is now a trend to using nano-sized particles as the additional ingredient of the nickel composite. Wu et al. [21] reported that the Al_2O_3 nanopowder addition into the plating solution

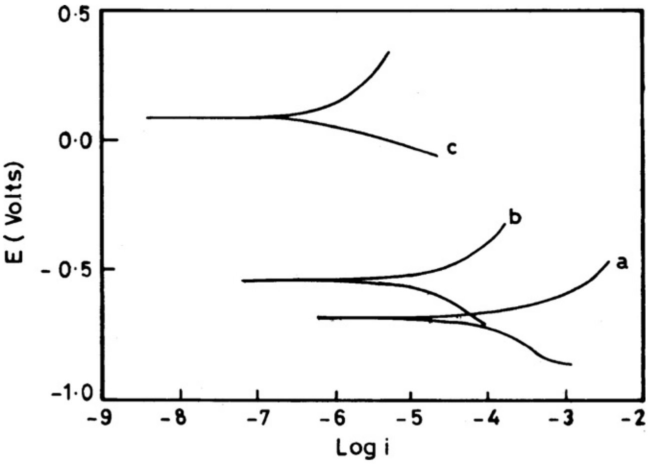

Fig. 8. Polarization studies of (a) blank MS, (b) sputtered Ni on MS and (c) brush plated Ni on MS in 3.5% w/v NaCl.

Table 5
Corrosion parameters obtained from polarization studies in 3.5% w/v NaCl

Sample	E_{corr} vs SCE (mV)	b_a (mV/dec)	b_c (mV/dec)	I_{corr} (A/cm^2)	Corrosion rate (mpy)
MS panel	−0.680	0.118	−0.196	1.26×10^{-4}	0.57×10^{-4}
Sputtered Ni on MS	−0.542	0.177	−0.201	1.80×10^{-5}	0.76×10^{-5}
Brush plated Ni on MS	+0.087	0.212	0.091	7.25×10^{-7}	3.07×10^{-7}

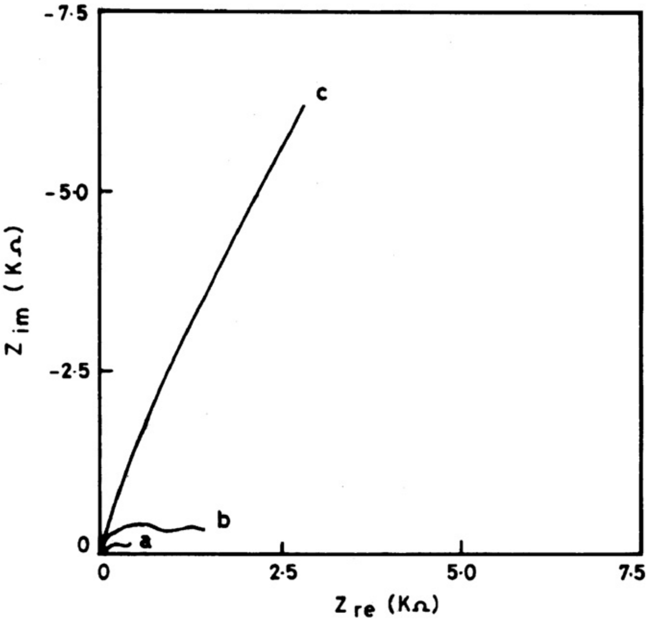

Fig. 9. Nyquist plots for corrosion measurements of (a) blank MS, (b) sputtered Ni film and (c) brush plated Ni film on MS in 3.5% w/v NaCl.

increased the coating micro hardness, particularly for nickel based coatings.

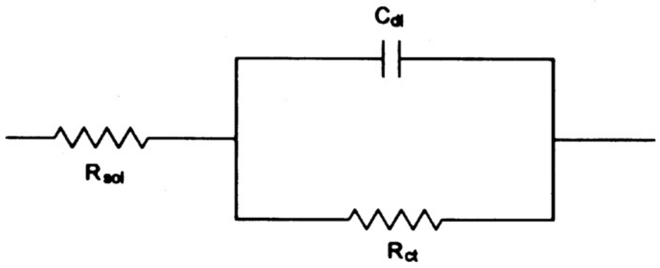

Fig. 10. Equivalent circuit for a corroding metal.

Table 6
Corrosion parameters obtained from impedance measurements by Nyquist plots

Sample	OCP (V)	R_{ct} (Ω cm^2)	C_{dl} (F/cm^2)
MS Panel	−0.655	93.8	5.616×10^{-3}
Sputtered Ni on MS	−0.506	1032.8	1.408×10^{-5}
Brush plated Ni on MS	+0.148	5937.4	8.702×10^{-7}

4. Conclusions

A comparison between sputtered and brush plated Ni was made in this study. The sputtered Ni film showed better crystallinity as observed from XRD compared to brush plated Ni film on steel on account of the favorable conditions for grain growth in sputtering. A higher microhardness values of sputtered Ni film compared to brush plated Ni film is because of the high residual stress from the sputter process. The coating thickness for brush plated Ni shows a parabolic relationship with time while that for sputtered Ni is linear. This is because of the diffusion controlled process in the plating bath for brush plating whereas bombardment and momentum transfer in the case of sputter process. The corrosion rate observed on brush plated Ni film sample was significantly lower than that of the sputtered Ni film.

Acknowledgement

One of the authors (B.S.) thanks the Department of Science and Technology, New Delhi, for a research grant under SERC Fast Track Scheme No. SR/FTP/CS-23/2005.

References

[1] R.A. Mirshams, P. Parakala, Mat. Sci. Eng. A 372 (1–2) (2004) 252.
[2] M. Bin-Sudin, A. Leyland, A.S. James, A. Mathews, J. Housden, B. Garside, Surf. Coat. Technol. 81 (1996) 215.
[3] T. Tuken, A.T. Ozylmaz, B. Yazici, C. Kardos, M. Erbil, Prog. Org. Coat. 51 (1) (2004) 27.
[4] H. Mu, J. Seok, R.Y. Lin, J. Electrochem. Soc. 150 (2) (2003) C67.
[5] L.L. ShreirCorrosion, 2, Newness-Butter worths, London Boston, 1976.
[6] L. Du, B. Xu, S. Dong, H. Yang, Y. Wu, Surf. Coat. Technol. 192 (2005) 311.
[7] W.H. Hui, J.J. Liu, Y.S. Chang, Surf. Coat. Technol. 68–69 (1994) 546.
[8] J.W. Dini, Met. Finish. 95 (6) (1997) 88–93.

[9] B. Subramanian, C. Sanjeeviraja, M. Jayachandran, Sol. Energy Mat. Sol. Cells 79 (2003) 57.
[10] K. Bouslykhane, J.P. Villain, P. Moine, Tribol. Int. 29 (1996) 169.
[11] J.C. Doong, J.G. Duh, S.Y. Tsai, Surf. Coat. Technol. 58 (1993) 51.
[12] K. Singh, A.K. Gover, M.K. Totlani, A.K. Suri, Trans. Inst. Met. Finish. 78 (1) (2000) 23.
[13] M. Irie, H. Ohara, M. Tsujioka, T. Nomura, Mat. Chem. Phys. 54 (1998) 317.
[14] F. Bean Cou, J.J. hi, J.G. Duh, Thin Solid Films 377–378 (2000) 354.
[15] X.W. Zhou, H.N.G. Wadley, S. Sainathan, Nucl. Instrum. Meth. B 234 (4) (2005) 441.
[16] Y. Milkami, K. Yamada, A. Ohnari, T. Degawa, T. Migiba, T. Tanaka, K. Kawbata, H. Kajioka, Surf. Coat. Technol. 133 (2000) 295.
[17] S.H. Kim, U. Erb, K.T. Aust, F. Gonzalez, G. Palumbo, Plat. Surf. Finish. 5 (2004) 68.
[18] Haichuan Mu, Jin Seok, R.Y. Lin, J. Electrochem. Soc. 150 (2) (2003) C67.
[19] S. Velumani, H. Castaneda, U. Pal, J.V. Chavez, P.J. Sebastian, J.A. Ascencio, J. Solid State Electrochem. 9 (2005) 535.
[20] G. Venkatachari, Corros. Bull. 2 (5) (1982) 14.
[21] Bin Wu, Bin-shi Xu, Bin Zhang, Xue-dong Jing, Cun-long Liu, Mat. Lett. 60 (13–14) (2006) 1673.